Interpretation of helium charge exchange spectra for transport studies in fusion plasmas

A. Kappatou[1], R.M. McDermott[2], R.J.E. Jaspers[3], T. Pütterich[2], R. Dux[2]

and the ASDEX Upgrade team

[1] *FOM Institute DIFFER-Dutch Institute for Fundamental Energy Research, Association EURATOM-FOM, Nieuwegein, The Netherlands.*

[2] *Max-Planck-Institut für Plasmaphysik, EURATOM Association, Garching, Germany.*

[3] *Science and Technology of Nuclear Fusion, Eindhoven University of Technology, Eindhoven, The Netherlands.*

The helium plume effect

The helium "plume" effect [1] has a strong impact on the analysis of the measured charge exchange (CX) spectra. The plume emission originates from the He^+ particles created through CX reactions along the neutral beam path. These particles follow the magnetic field lines and can cross the lines-of-sight (LOS) of the CX diagnostic before being reionised. There, due to electron impact excitation, these hydrogenic plume ions may emit additional photons, causing an additional contribution to the measured CX signal. The helium plume signal is superimposed and of comparable magnitude to the active CX (prompt) signal. As such, it disturbs the measurements and leads to overestimation of the He^{2+} density.

The non-local plume emission cannot be distinguished from the prompt CX signal or subtracted from the helium CX spectra using a neutral beam modulation scheme. Furthermore, the plume emission depends strongly on the observation geometry of the diagnostic, but also on the plasma parameters and the beam attenuation. It is, therefore, necessary that the plume emission be modelled, so as to enable accurate extraction of the active CX signal. Several attempts have been made in the past to model and understand the plume effect [1]-[3]. Here a detailed model for the helium plume effect for ASDEX Upgrade is presented, which includes a Monte Carlo beam attenuation model, a full, accurate 3-D geometry and reconstruction of the magnetic equilibrium and takes into account the plasma rotation and Maxwellian velocity distribution of the plume ions. Helium CX spectra obtained at ASDEX Upgrade are analysed and corrections to He^{2+} density profiles are derived and the results are compared with experimental data from two different diagnostic observation geometries.

Modelling of the helium plume effect

The modelling of the helium plume emission entails the solution of the continuity equation for the transport of He^+ ions along the field lines. The source of the hydrogen-like plume ions is the CX of fully ionized helium ions with the beam neutrals and the loss mechanism is the ionisation process.

The first step is to evaluate the source of plume ions in the beam volume. The beam neutrals can be calculated either using FIDASIM, a Monte Carlo code that models the density of the beam and beam halo neutrals [5], or derived from beam emission spectroscopy (BES). An

initial He^{2+} density profile is assumed and the total CX cross-sections are used to calculate the source of plume ions. The loss of the plume ions at a given location in the plasma is evaluated using the ionisation rate coefficients due to electron impact. For typical plasma parameters, for example $T_e = T_i = 2keV$ and $n_e = 8 \cdot 10^{19} m^{-3}$, the electron impact ionisation length for He^+ is $\lambda_i = \upsilon_{th}(T_i) \cdot n_e^{-1} \cdot q_{ion,e}(T_e, n_e)^{-1} = 0.47m$, where $\upsilon_{th}(T_i) = \sqrt{(2 \cdot k \cdot T_i)/(\pi m)}$ while $\tau_{ion}^{-1} = n_e \cdot q_{ion}^e(T_e, n_e)$ is the ionisation time and $q_{ion}^e(T_e, n_e)$ is the electron impact ionisation rate coefficient. All atomic data are taken from [6].

Once the source term is known the next step is to reconstruct the magnetic equilibrium and to follow the plume ions along the magnetic field lines (assuming no perpendicular flows), to their intersection points with the diagnostic LOS. The density of plume ions along the magnetic field lines is obtained by solving the steady state continuity equation for ions moving along the field lines in both directions. The plume ions are assumed to be born with the same full velocity distribution as He^{2+}, taking into account the plasma rotation.

The helium plume emission along a diagnostic LOS is determined using the local electron impact excitation rate coefficient for photon emission at the wavelength of interest (HeII (n=4-3), 468.571nm). For these calculations, ion temperature and rotation profiles from the B^{5+} (n=7-6) CX line have been used, as the plume effect is negligible for boron.

The code also calculates the expected prompt CX emission based on the initially assumed He^{2+} density, using the cross-sections for charge exchange of He^{2+} (n=4-3) with the neutral beam. In this way the ratio of the plume to active CX emission can be determined.

Benchmarking of the model with experimental data

A validation of the model for the helium plume described in the previous section with experimental data has been undertaken.The model has been used to compute the active CX and plume emission signals for an ASDEX Upgrade discharge (29083).

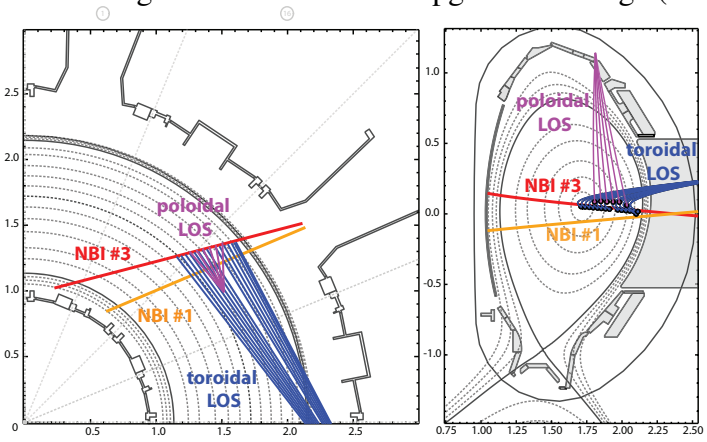

Figure 1: Top down and poloidal view of ASDEX Upgrade, with the geometry of the two sets of lines-of-sights and the two beam sources used in the experiment.

The helium spectrum was measured using a high optical throughput spectrometer suitable for core charge exchange measurements on ITER [4], currently utilised on ASDEX Upgrade. For this discharge, the spectrometer was connected to two optical heads: one with purely toroidal LOS and one with more poloidal LOS, all focussed on neutral beam #3 (see Fig. 1). For an additional check, NBI #3 was replaced by NBI #1, for several phases of the plasma discharge. NBI #1 (also shown in Fig. 1) is more radial than NBI #3 and is situated below the toroidal LOS.

The calculated plume-to-prompt ratios for discharge 29083 from two time points (t=2.555s when NBI #3 is on and t=2.945s when NBI #1 is on) are shown in Fig. 2 for the two viewing geometries. The dashed lines correspond to a modelling of the plume emission assuming that all plume ions have a single velocity equal to the mean thermal velocity, while for the solid lines a full Maxwellian velocity distribution has been used. A comparison of the two methods as well as an illustration of the spread of the plume emission along the LOS, in comparison to the prompt CX emission, can be seen in Fig. 3, for the two innermost LOS of each optical head. The two methods agree quite well for the poloidal LOS, however, there is a disagreement for the toroidal LOS. The plume emission seen by the poloidal LOS comes almost exclusively from the intersection of these LOS with the neutral beam. The toroidal LOS, on the other hand, are almost tangential to the magnetic field lines at the beam location and collect plume emission not only from the beam intersection, but also from immediately adjacent volumes. In these regions, the full velocity distribution method models the plume emission more accurately, as the particles with velocities lower than the mean thermal velocity, which remain in the vicinity of the neutral beam, are better described. Nevertheless, the disagreement between the two methods can be up to a factor of 2, as rotation goes to zero.

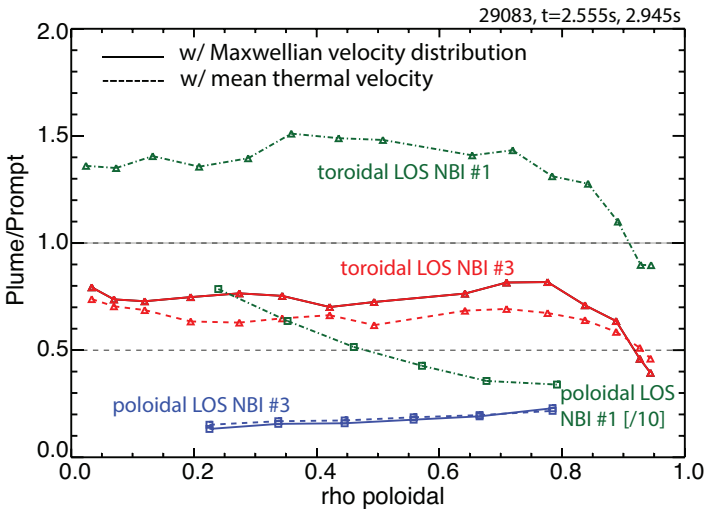

Figure 2: The ratio of the plume to prompt emission for the two sets of lines-of-sight of the diagnostic for ASDEX Upgrade discharge 29083 at 2.555s and 2.945s, as calculated from the plume model.

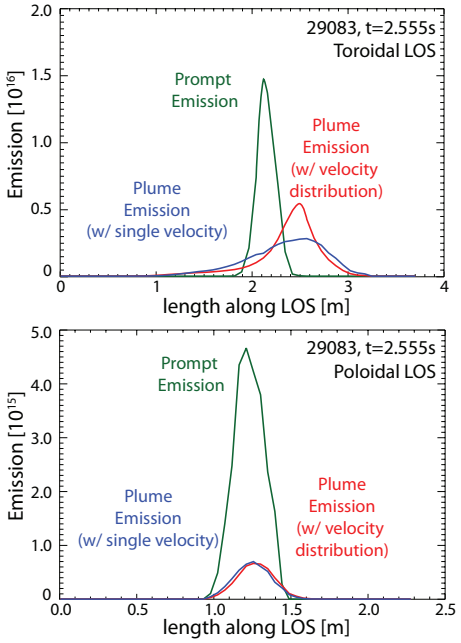

Figure 3: Plume emission along a LOS for the toroidal and poloidal viewing geometries.

As expected, the plume emission collected by the poloidal LOS is from the same location as the prompt CX signal, while the toroidal LOS collect emission from the hydrogenic plume ions from a broader region.

The plume-to-prompt ratio for the toroidal LOS when NBI#3 is on is higher than the corresponding ratio for the poloidal LOS, as the path of the poloidal LOS through the plume cloud is smaller than for the toroidal LOS. The situation changes when NBI #1 is on instead. The toroidal LOS are above the center of NBI #1 and only view the edge of this source. As such, the prompt CX signal is lower for the toroidal LOS (by approximately a factor of 3 in the core). However, the toroidal LOS still measure plume ions produced by NBI #1 which have followed the magnetic field lines

into the LOS. In this case, the plume-to-prompt ratio is almost a factor of 2 higher than for NBI #3. The poloidal LOS barely intersect NBI #1 and measure almost exclusively the plume originating from NBI #1. The calculated plume-to-prompt ratio is indeed approximately 10 times higher in comparison to the ratio for the NBI #3 time point (shown divided by 10 in Fig. 2).

In Fig. 4, the He^{2+} density profiles derived without taking into account the plume effect are shown on the left for both sets of LOS. As the lines-of-sight have different geometries in relation to the magnetic field lines and the neutral beam and are therefore affected by the plume differently, the experimental density profiles from the three sets of data do not agree. In the right plot, however, the plume-corrected density profiles are shown. The corrected densities are obtained by multiplying the densities on the left plot with a factor of $1/(1+\mathrm{R})$, where R is the ratio of plume emission signal integrated along each LOS to the active CX signal, shown in Fig. 2. In this case, the plume-to-prompt ratio was calculated using the Maxwellian velocity distribution method. The corrected density profiles from the toroidal and the poloidal LOS are now in much better agreement. In addition, as the plasma parameters are similar between the NBI #1 and NBI #3 phases, the He^{2+} density profile from the NBI #1 phase can be compared to the profile measured on NBI #3. Very good agreement is found in this case as well.

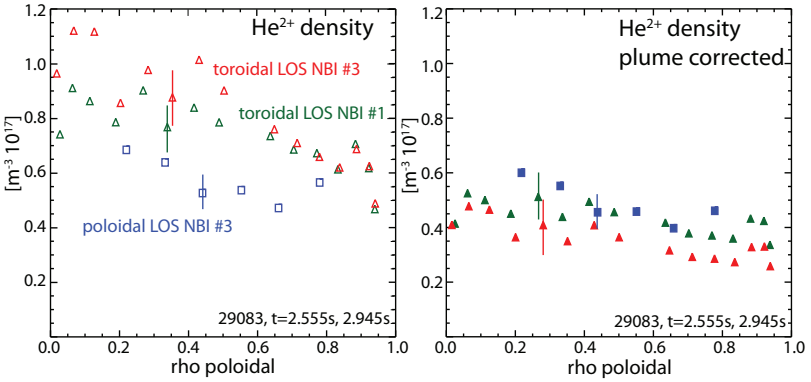

Figure 4: He^{2+} density profiles obtained from CX measurements for the ASDEX Upgrade discharge 29083 at 2.555s (NBI #3 on) and at 2.945s (NBI #1 on) without the plume effect taken into account and the corrected profiles after the plume effect has been modelled, for the toroidal and poloidal viewing geometry.

Discussion

An analytic model for the helium plume emission has been implemented for ASDEX Upgrade. It is shown that the plume corrections to the helium densities extracted from HeII CX are roughly a factor of 2 and can not be neglected. Here, the use of two separate viewing geometries for CX measurements, on two differently oriented neutral beams, helps to validate the assumptions of the forward modelling of the plume emission. Comparison with experimental data is at this stage very encouraging, but further analysis of the model is still required.

References

[1] R.J. Fonck *et al*, Phys. Rev. A **29**, 3288 (1984)
[2] U. Gerstel *et al*, Plasma Phys. Control. Fusion, **39**, 737 (1997)
[3] D.F. Finkenthal, PhD thesis, University of California at Berkeley (1994)
[4] R.J.E. Jaspers *et al*, Rev. Sci. Instrum. **83**, 10D515 (2012)
[5] B. Geiger, PhD thesis, Ludwig-Maximilians-Universität München (2012)
[6] H.P. Summers, ADAS User Manual 2.6 (2004), http://www.adas.ac.uk/manual.php